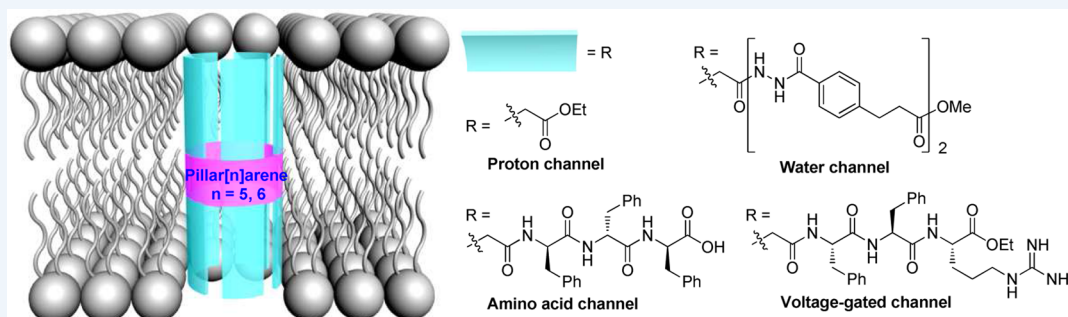


## Tubular Unimolecular Transmembrane Channels: Construction Strategy and Transport Activities

Wen Si, Pengyang Xin, Zhan-Ting Li, and Jun-Li Hou\*

Department of Chemistry, Fudan University, 220 Handan Road, Shanghai 200433, China



**CONSPECTUS:** Lipid bilayer membranes separate living cells from their environment. Membrane proteins are responsible for the processing of ion and molecular inputs and exports, sensing stimuli and signals across the bilayers, which may operate in a channel or carrier mechanism. Inspired by these wide-ranging functions of membrane proteins, chemists have made great efforts in constructing synthetic mimics in order to understand the transport mechanisms, create materials for separation, and develop therapeutic agents.

Since the report of an alkylated cyclodextrin for transporting  $\text{Cu}^{2+}$  and  $\text{Co}^{2+}$  by Tabushi and co-workers in 1982, chemists have constructed a variety of artificial transmembrane channels by making use of either the multimolecular self-assembly or unimolecular strategy. In the context of the design of unimolecular channels, important advances have been made, including, among others, the tethering of natural gramicidin A or alamethicin and the modification of various macrocycles such as crown ethers, cyclodextrins, calixarenes, and cucurbiturils. Many of these unimolecular channels exhibit high transport ability for metal ions, particularly  $\text{K}^+$  and  $\text{Na}^+$ .

Concerning the development of artificial channels based on macrocyclic frameworks, one straightforward and efficient approach is to introduce discrete chains to reinforce their capability to insert into bilayers. Currently, this approach has found the widest applications in the systems of crown ethers and calixarenes. We envisioned that for macrocycle-based unimolecular channels, control of the arrangement of the appended chains in the upward and/or downward direction would favor the insertion of the molecular systems into bilayers, while the introduction of additional interactions among the chains would further stabilize a tubular conformation. Both factors should be helpful for the formation of new efficient channels.

In this Account, we discuss our efforts in designing new unimolecular artificial channels from tubular pillar[n]arenes by extending their lengths with various ester, hydrazide, and short peptide chains. We have utilized well-defined pillar[5]arene and pillar[6]arene as rigid frameworks that allow the appended chains to afford extended tubular structures. We demonstrate that the hydrazide and peptide chains form intramolecular  $\text{N-H}\cdots\text{O}=\text{C}$  hydrogen bonds that enhance the tubular conformation of the whole molecule. The new pillar[n]arene derivatives have been successfully applied as unimolecular channels for the selective transport of protons, water, and amino acids and the voltage-gated transport of  $\text{K}^+$ . We also show that aromatic hydrazide helices and macrocycles appended with peptide chains are able to mediate the selective transport of  $\text{NH}_4^+$ .

### 1. INTRODUCTION

Cell membranes are mainly composed of phospholipids, such as phosphatidylcholine, phosphatidylethanolamine, phosphatidylserine, and sphingomyelin. The interior of their bilayer structure is hydrophobic and compact. As a result, ions and polar molecules cannot pass freely. Nature has evolved membrane protein channels to move them across the membrane. These channel proteins are also critical for cellular regulation, intercellular communication, and mediation of electrical excitability of the nervous and muscle systems.<sup>1</sup> Because of their extreme importance in life, chemists have a

long-term interest in constructing artificial channels. The study of artificial channels is not only aimed at gaining insight into the mechanism of natural channels<sup>2</sup> but also can potentially lead to new therapeutic, separation and purification, and sensing technologies.<sup>3</sup> This is also an important research field in supramolecular chemistry<sup>4</sup> because the insertion of a channel into a bilayer and the subsequent transmembrane transport is a

Received: March 24, 2015

Published: May 27, 2015

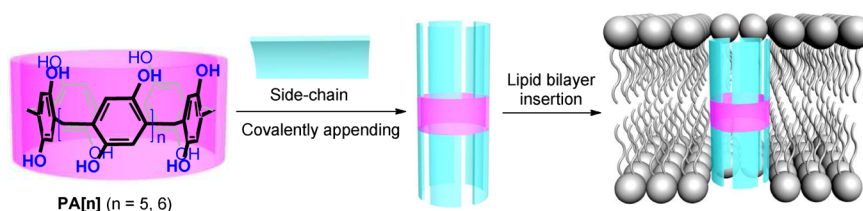


**Figure 1.** Schematic representation of our strategy for the construction of unimolecular tubular channels from PA[*n*]s (*n* = 5, 6).

typical dynamic process within a complicated self-assembled system.

In the last three decades, chemists have constructed a large number of artificial channels,<sup>5</sup> which may be roughly divided into two categories: self-assembled and unimolecular systems. The self-assembled channels are composed of two or more molecular components that are held together by non-covalent forces.<sup>6–8</sup> The components are usually structurally simple.<sup>9–12</sup> Nevertheless, the characterization of their supramolecular structures and transport molecularity in the bilayer may be a challenge, and for some of the supramolecular systems, attaining an essential concentration of the self-assembled transporters in the bilayer requires a high concentration of the component molecules. Unimolecular channels are usually structurally more complicated, and thus, their preparation may require multistep synthesis. However, the unimolecular feature can allow for straightforward structural characterization and more accurate manipulation of the transporter in the bilayer. Representative successful examples include covalently linked gramicidin A (gA)<sup>13–15</sup> and alamethicin (AL),<sup>16,17</sup> tethered<sup>18</sup> or tandem-linked crown ethers,<sup>19–21</sup> side-chain-attached crown ethers,<sup>22,23</sup> cyclodextrins,<sup>24</sup> calixarenes,<sup>25,26</sup> and cucurbiturils.<sup>27</sup> Many of these unimolecular channels can exhibit high transport ability for metal ions, particularly K<sup>+</sup> and Na<sup>+</sup>.<sup>28–30</sup>

In biological systems, channel proteins adopt stable conformations to achieve high efficiency and selectivity. Our strategy for the construction of artificial channels is to build confined unimolecular tubular structures on the basis of their predictable conformation and high capacity of inserting into bilayers, probably in a controllable manner. The thickness of the hydrophobic part of the lipid bilayer is 3.0–3.5 nm. Thus, the creation of a single tubular molecule that is long enough to span the bilayer has been a challenge.<sup>31</sup> Pillar[*n*]arenes (PA[*n*]s) are a new class of macrocycles that have rigid backbones composed of hydroquinone units linked at the para positions with methylene units.<sup>32–35</sup> We envisioned that this family of rigid molecular tubes might be new useful frameworks for the construction of longer tubular structures by attachment of linear segments of tunable length (Figure 1). Their symmetric pillar-styled structural feature would also favor the formation of straight or extended unimolecular tubes for the passage of ions and small organic molecules. Moreover, the introduction of non-covalent interactions, such as hydrogen bonding, among the attached segments was expected to further enhance the stability of the tubular conformations. These advantages join together to endow this new generation of unimolecular channels with robust capacity to transport both ions and neutral species in a selective and/or controllable manner.

## 2. PROTON CHANNEL

Our motivation for the construction of PA-based artificial channels originated from the crystal structure of decaester **1**.<sup>36</sup>

We found that this ester-attached PA[5] derivative adopted a tubular conformation and stacked cofacially to form infinite uniform organic tubes in the solid state. In particular, the tubes contained water molecules that were arranged into single wires associated by continuous hydrogen bonds (Figure 2). Although

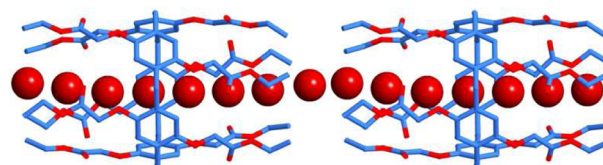
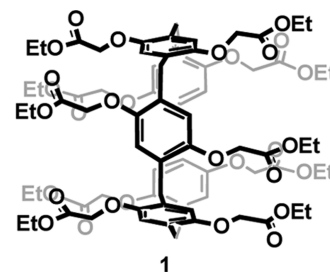


**Figure 2.** Crystal structure of compound **1**. The O atoms of the entrapped water molecules are highlighted using CPK spheres. H atoms have been omitted for clarity.

the ester groups are good hydrogen-bond acceptors, no hydrogen bonds were formed between them and the entrapped water molecules, reflecting the high strength of the hydrogen bonds formed within the entrapped water molecules. This unique pore–water wire hybrid was fascinating to us because to some extent it mimicked the structural features of natural proton channels that are closely related to the cross-membrane bioenergetics of cells.<sup>37</sup>



We further found that **1** could be incorporated into planar lipid bilayers to serve as proton channels, which was evidenced by the flux of protons across the bilayer in patch clamp experiments in hydrochloric acid solution (HCl/H<sub>2</sub>O) (Figure 3a).<sup>38</sup> However, after addition of **1** to the hydrochloric acid solution, the experiments showed quite low partitioning of this molecule into the hydrochloric acid solution because of its low water solubility. This low partitioning led to its low membrane-incorporation capability and difficulty in determining the molecularity as a proton channel. The length of **1** in the extended state is ca. 1.6 nm. On the basis of the thickness of the hydrophobic part of the bilayer, we conjectured that two molecules of **1** might combine to form a transmembrane channel, which would allow the formation of a water wire in its interior.

The conductance ( $\gamma$ ) of **1** in solution reflects the proton transport rate constant. Thus, the ratio of  $\gamma$  in HCl/H<sub>2</sub>O to that in DCl/D<sub>2</sub>O represents the kinetic proton transport isotope

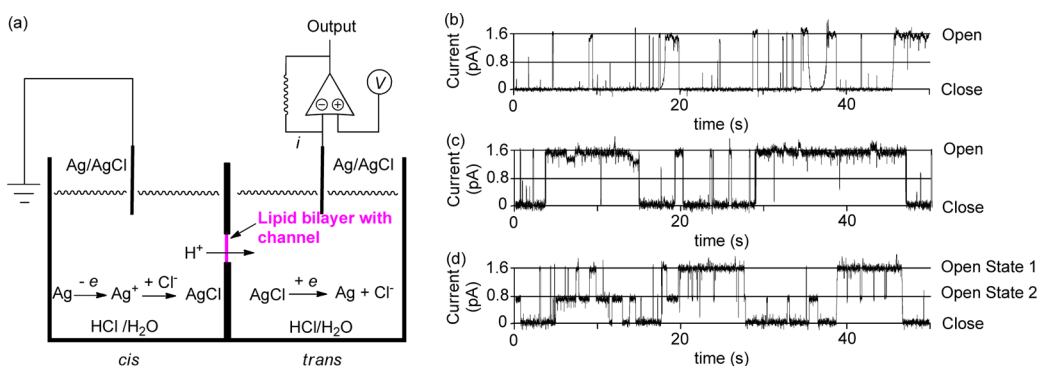
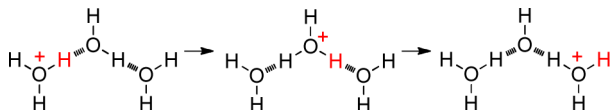


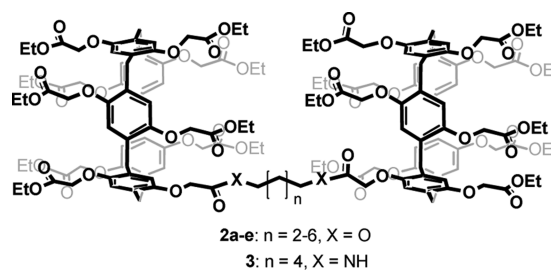
**Figure 3.** Patch clamp experiments on planar lipid bilayer. (a) Schematic representation of the experimental setup. The lipid bilayer was formed by painting the lipid in *n*-decane around an aperture. Then a solution of the channel in dimethyl sulfoxide was added to the *cis* chamber. The channel molecules could insert into the bilayer driven by hydrophobic interactions. When a voltage was applied across the bilayer, currents would be detected if the molecules formed transmembrane channels. The redox reactions on both Ag/AgCl electrodes are inserted to illustrate the nature of charge balance during proton transport. (b–d) Current traces (+40 mV) of **1**, **2c**, and **3** in the planar lipid bilayer in hydrochloric acid solution (pH 4.4). Reproduced with permission from ref 38. Copyright 2011 Wiley-VCH Verlag GmbH and Co. KGaA, Weinheim.

effect, which gave us insight into the proton transport mechanism. The patch clamp experiments in DCl/D<sub>2</sub>O solution did reveal a reduced conductance compared with that in HCl/H<sub>2</sub>O solution because of the higher dissociation energy of the O–D bond in comparison with the O–H bond. From the ratio of  $\gamma_{\text{HCl}/\text{H}_2\text{O}}$  to  $\gamma_{\text{DCl}/\text{D}_2\text{O}}$ , the proton transport isotope effect was determined to be 1.6. This primary isotope effect demonstrated that the dissociation of O–H bonds was involved in the proton transport process. The dissociation of an O–H bond led to the rearrangement of the hydrogen bonds of two adjacent water molecules, causing the migration of a proton from one water molecule to the next one.<sup>39</sup>



Encouraged by the above observations, we prepared compounds **2a–e** by connecting two PA[5] units with an aliphatic linker.<sup>38</sup> As expected, all of these compounds transported protons, but their activities were different. Compound **2c**, whose two PA[5] units are connected by a hexamethylene linker, exhibited the highest activity, which we attributed to the best-matched face-to-face stacking of the two PA[5] units. The shorter or longer spacers in compounds **2a**, **2b**, **2d**, and **2e** were less favorable for such face-to-face stacking of the linked PA[5] units. The open probability of unimolecular channel **2c** was 2 times higher than that of the bimolecular channel formed by **1** (Figure 3b,c), indicating that the former was more stable than the latter. The proton transport isotope effect of **2c** was identical to that of the channel formed by **1**, indicating that proton transport by **2c** also proceeded through the water wire formed in the PA[5] units. As the water wire provided a specific track for the migration of protons, a high selectivity for protons over Cl<sup>−</sup> could be achieved. Highly selective artificial proton transport was first constructed by Matile and co-workers through continuous hydrogen-bonded hydroxyl chains formed by a polyol.<sup>40</sup> However, this new proton transport through water wires provides a more straightforward mimic of natural proton channels such as influenza A M2 protein.<sup>41</sup>

Channel **3**, whose two PA[5] units are connected by hexane-1,6-diamine, also exhibited transport activity for protons.<sup>38</sup>



However, in contrast to **1** and **2c**, which displayed one transport state, **3** showed two transport states (Figure 3d). One state (state 1) originated from proton transport along the water wire, as revealed by its isotope effect, which was close to those of **1** and **2c**. The other state (state 2) showed a lower conductance and a higher isotope effect than the first one, which was attributed to the existence of the two amide groups in **3** and exchange of the hydrogen atoms with neighboring water molecules. The exchange of the hydrogen atoms significantly decreased the proton transport rate, as shown by the substantially lower conductance of state 2 compared with state 1.

### 3. WATER CHANNEL

We further prepared longer compounds **4** and **5** by attaching hydrazide chains to both sides of the PA[5] backbone.<sup>42</sup> The crystal structure of compound **4** (Figure 4) and its <sup>1</sup>H NMR spectra in chloroform showed that the adjacent hydrazide subunits could form intramolecular hydrogen bonds, which should promote the formation of the tubular structure by the hydrazide chains. The crystal structure of **4** also showed that hydrogen-bonded water dimers existed within the hydrophilic hydrazide regions (Figure 4). The water dimers were hydrogen-bonded to the carbonyl O atoms of the adjacent hydrazide subunits. Within the hydrophobic regions formed by the PA[5] and benzene rings, water was absent. Thus, no continuous water wire was formed.

The length of extended **5** is about 5.0 nm, which is long enough to span the lipid bilayer. Upon mixing of **5** with lipid vesicles containing NaCl (100 mM), the high hydrophobicity of the molecules did drive them to spontaneously insert into the vesicle bilayer to form a channel. The tubular conformation was expected to be maintained because the nonpolar environment of the bilayer was favorable for the formation of hydrogen

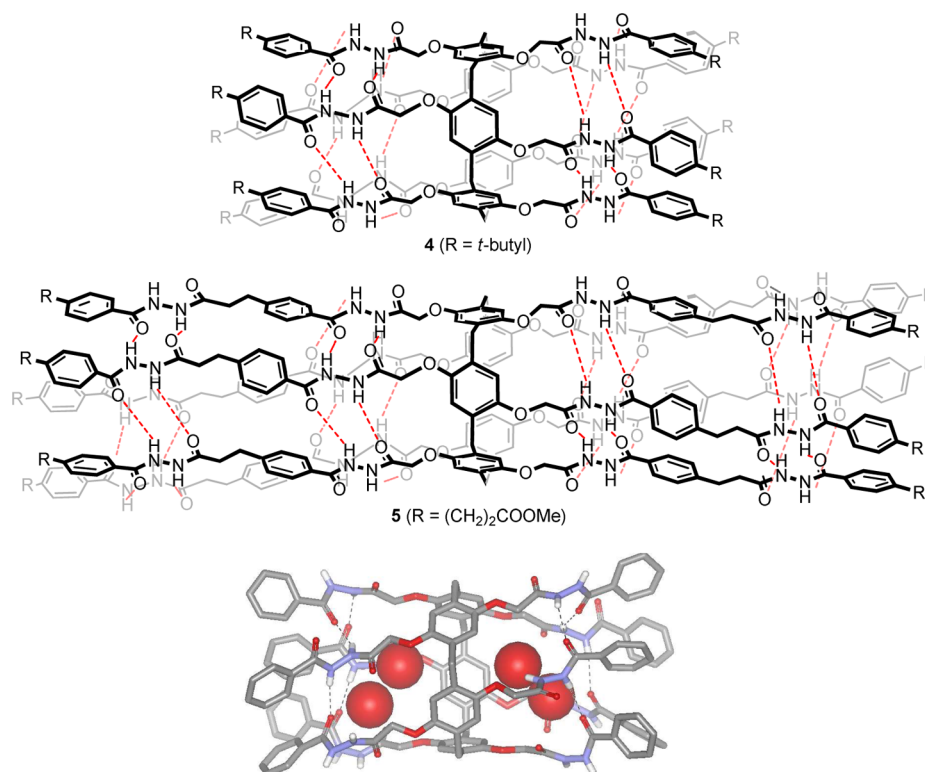


**Figure 4.** (top) Chemical structures of compounds **4** and **5**. (bottom) Crystal structure of **4** (stick model). The O atoms of four entrapped water molecules are highlighted using CPK spheres. The *tert*-butyl groups and H atoms on the C atoms have been omitted for clarity. Reproduced from ref 42. Copyright 2012 American Chemical Society.

bonds between the hydrazone subunits. The squeezing of the surrounding lipid molecules should further promote the approach of the side chains and thus stabilize the tubular structure. Driven by the osmotic pressure difference between the outside and inside of the vesicles, water could flux through the channels (Figure 5a), which led to swelling of the vesicles

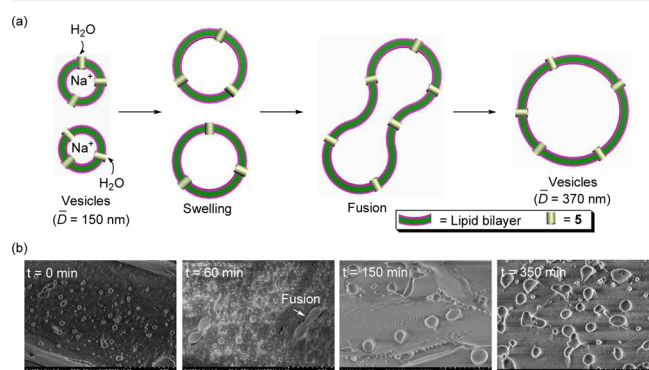


**Figure 5.** (a) Schematic representation of the increase in vesicle size caused by **5**-mediated outside-to-inside water transport. (b) cryo-SEM images of the vesicle sample after addition of **5**. Reproduced from ref 42. Copyright 2012 American Chemical Society.

and their subsequent fusion into larger vesicles, as indicated by cryogenic scanning electron microscopy (cryo-SEM) experiments (Figure 5b). The transport showed a first-order dependence on the concentration of **5**, indicating that it performed as a unimolecular channel. The water permeability was determined to be  $8.6 \times 10^{-10}$  cm/s or 40 water molecules per second, which is about 6 orders of magnitude lower than

that of natural water channel aquaporin. However, the actual value was likely to be higher than this measured one because most of the channel molecules were not inserted into the bilayer. The high water permeability is related to the unique noncontinuous water wire, which allowed water molecules to move freely.

In natural systems, the water channel aquaporin can block proton transport during the water transport process, which is one of the important features of aquaporin in regulating the cellular microenvironment.<sup>43</sup> Similar to aquaporin, the artificial unimolecular water channel **5** was also able to block proton transport across the lipid bilayer through the formation of a noncontinuous water wire within its cavity. Thus, a high transport selectivity of water over protons was achieved, and **5** represents the first example of an artificial channel that mimics this function of aquaporin. This result shows that the structural disruption of the water wire within a channel could be a reliable method for controlling the water/proton selectivity in the future design of new channels, although in aquaporin the control of this selectivity is based on the reverse-flip net-dipolar water wire profiles.<sup>44</sup>

#### 4. AMINO ACID CHANNEL

By attaching short Phe tripeptide chains to the backbone of PA[5] or PA[6], we also prepared PA[5] derivative **6a** and PA[6] derivative **6b**.<sup>45</sup> Although the corresponding PA[5] and PA[6] precursors are racemic, all of these peptide-appended compounds were obtained in an optically pure state, as indicated by their <sup>1</sup>H NMR spectra, which displayed one set of signals. This occurs because the chiral peptide chains induce the racemic PA backbones to convert into one of the two isomers. The chirality of this isomer matched better with the attached

chiral peptide chains, and thus, the resulting products were lower in energy. The D-L-D ordering of residues was chosen for the peptide chains because molecular modeling showed that for tubular structures formed by these PA derivatives, all of the side chains of the amino acid residues in this ordering could be oriented to the outside surface of the tube (Figure 6). Similar to

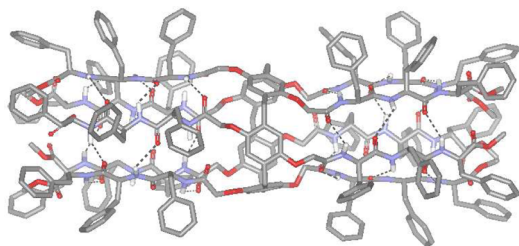
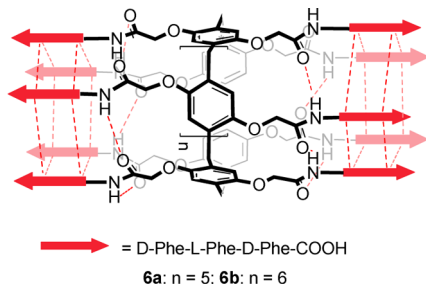


**Figure 6.** Structure of **6a** obtained by molecular modeling (Gaussian 09, semiempirical, PM6). H atoms on the C atoms have been omitted for clarity. Reproduced from ref 45. Copyright 2013 American Chemical Society.

the hydrazide-derived molecules, these compounds were also revealed to form intramolecular hydrogen bonds between the appended peptide chains. Although all of the channels with peptides of different length attached could form unimolecular channels in the bilayer, a systematic investigation revealed that the channel with tripeptides possessed the highest membrane-incorporation ability. This significantly high ability was ascribed to its length (3.2 nm), which was well-matched with the thickness of the hydrophobic part of the bilayer (3.5 nm). The hydrophobic Phe residues were favorable for the insertion of the channel molecules into the lipid bilayer. In addition, the hydrophilic terminal carboxylic acid groups of the channels might also enhance the membrane-incorporation ability of the channels.



At the very low concentration of 0.05 mol % relative to lipids, both **6a** and **6b** showed significant enhancement of the amino acid transport rates. Although amino acids could pass across the bilayer by a simple diffusion mechanism, the rate enhancement observed at this low concentration demonstrated their effectiveness in transporting amino acids. For both compounds, the Hill coefficient (an indicator of the molecularity of a channel molecule) was close to 1.0, which indicated that they transported amino acids by a unimolecular mechanism. PA[5]-derived **6a** favored the transport of small amino acids such as Gly and Ala, whereas PA[6]-derived **6b** could allow the flux of the larger ones such as Phe. In addition, **6b** displayed transport selectivity for amino acid enantiomers—the transport of the D isomers of Ala, Ser, Thr, Val, and Leu was notably faster than that for their L isomers, and this difference increased with increasing amino acid size (Figure 7). For Phe, however, **6b** could allow only the flux of the L isomer. This transport

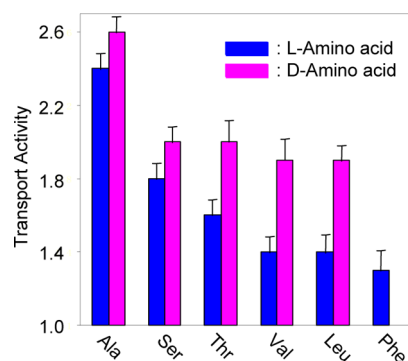
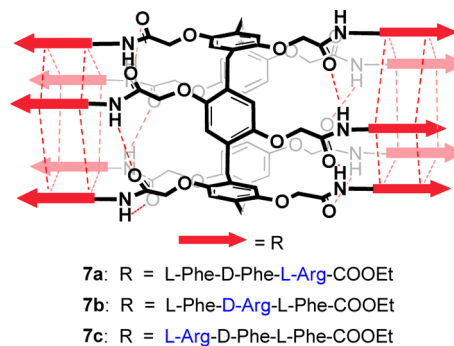


**Figure 7.** Transport activities of **6b** (0.05 mol % relative to lipids) for L and D-amino acids. Reproduced from ref 45. Copyright 2013 American Chemical Society.

selectivity for chiral amino acids is apparently due to the chirality of the cavity of the channels as a result of the chiral amino acid residues.

## 5. VOLTAGE-GATED CHANNEL

To further develop controllable channels, we screened the appended peptide chains and found that Arg-incorporated peptides could be used to design voltage-gated channels. We prepared compounds **7a–c**, the peptide chains of which consist of two neutral Phe residues and one positively charged Arg residue with different ordering.<sup>46</sup> Each of the three compounds contained a total of 10 positively charged Arg residues. These positively charged compounds were designed to mimic the S4 domain of natural voltage-gated K<sup>+</sup> channels, which contain four to eight Arg residues.<sup>47</sup>



Incorporation of hydrophilic Arg residues into the peptide chains and neutral ester groups at their ends led to a poor membrane-insertion capability for all three compounds, and thus, they could not insert into the lipid bilayer spontaneously. However, in the presence of a negative membrane potential, the membrane-insertion capability of **7a** was significantly increased, which could in turn depolarize the polarized-vesicle membrane, whereas a positive membrane potential had little effect on the membrane-insertion capability. Similar to the S4 domain, **7a** containing 10 end-located Arg residues could be forced to reversibly insert into and depart from the lipid bilayer by alternating application of voltages of  $-100$  and  $+100$  mV, respectively (Figure 8b), and thus switch transmembrane K<sup>+</sup> transport on and off, as demonstrated by patch clamp experiments on planar lipid bilayers (Figure 8a). Compounds **7b** and **7c**, in which the Arg residues are incorporated in the middle or interior of the chains, could also be driven to insert

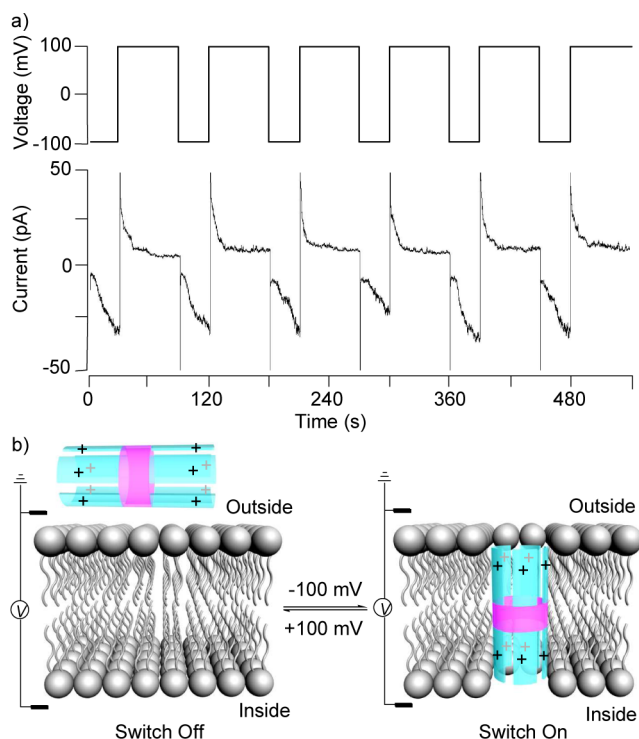


**Figure 8.** (a) Patch clamp macroscopic current trace (bottom) of **7a** under the alternating +100 and –100 mV voltage pulse protocol (top). (b) Schematic representation of voltage-driven channel insertion into and departure from the bilayer. Reproduced with permission from ref 46. Copyright 2014 Wiley-VCH Verlag GmbH and Co. KGaA, Weinheim.

into the bilayer. However, they did not leave reversibly from the bilayer, probably because of strong aggregation in the bilayer.

The gating charges of **7a–c** were determined to be 1.82, 2.70, and 1.64, respectively. These values were all higher than that of the natural voltage-gated channel melittin (1.5). The fact that **7b** displayed the highest gating charge indicates that it possessed the highest voltage-response capability. In addition to the above voltage-responsive behavior, **7b** also exhibited antimicrobial activity toward the Gram-positive bacteria *Bacillus subtilis* with an  $IC_{50}$  value of 10  $\mu$ M. This antimicrobial activity was attributed to its voltage-responsive behavior. Because the bacteria maintain a negative potential in their cell interior, **7b**, which possessed the highest voltage-response capability, was able to insert into the cell membrane and kill the bacteria by depolarizing the membrane. In contrast, **7a** and **7c** were less effective in killing the bacteria, consistent with their lower gating charges.

## 6. UNIMOLECULAR HELICAL CHANNEL

The above results showed that the Phe-based tripeptide chain is quite robust in enhancing the capacity of PA[n]-derived channels to insert into the lipid bilayer because of its strong hydrophobicity. We thus introduced the tripeptide chain on the helical aromatic hydrazide backbones that we had previously developed.<sup>48</sup> We prepared both oligomer **8** and polymer **9**, which have lengths of ca. 2.0 and 3.5 turns.<sup>49</sup> Both the oligomer and the polymer could insert into the lipid bilayer at low concentrations. The central helical aromatic hydrazide backbones produced a cavity of ca. 1.0 nm due to the intramolecular hydrogen bonds formed between the hydrazide NH subunits and the neighboring ether O atoms. We proposed that their

helical conformation should be maintained in the nonpolar bilayer. In a bulky solvent, the appended peptide chains should adopt flexible conformations (Figure 9a). However, upon

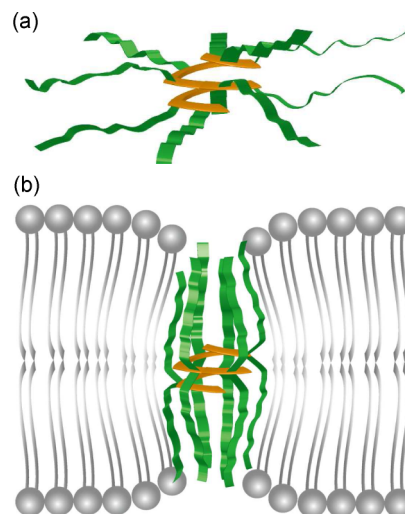
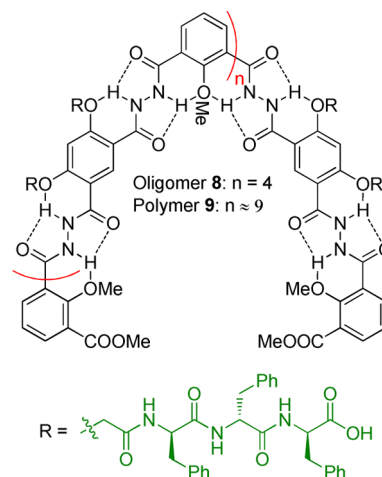


**Figure 9.** Schematic representations of (a) the structures of **8** and **9** with extended peptide chains and (b) the “squeezed” unimolecular channels formed by **8** and **9** in the bilayer. Reproduced from ref 49. Copyright 2014 American Chemical Society.

insertion into the bilayer, they were expected to aggregate from the two sides of the rigid helical backbones as a result of the squeezing effect of the surrounding lipid molecules (Figure 9b). Such arrangement of the peptide chains would lead to the formation of a “squeezed” unimolecular channel. The terminal carboxylic acid groups of the channel molecule would further serve as anchors to stabilize the channel–bilayer complex.



Patch clamp experiments revealed that oligomer **8** and polymer **9** could transport alkali-metal ions and  $NH_4^+$  across the lipid bilayer. The durations of the open signals observed in the patch clamp current traces were up to 15 s (Figure 10), which implied that the active conformers were quite stable in the bilayer. Further dynamic transport experiments indicated that the transport proceeded by a unimolecular mechanism. This result also excluded the possibility that these two compounds adopted an extended flat conformation in the bilayer. In this conformation, they should not be able to mediate the transport of the cations. Thus, we proposed the

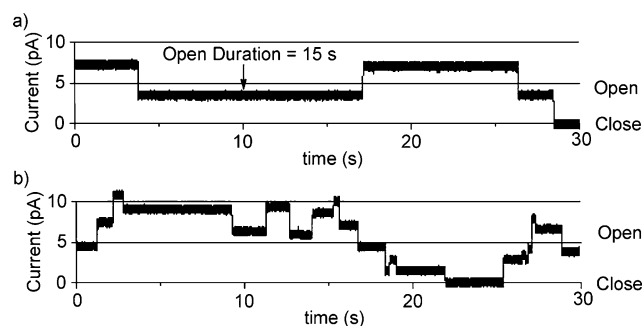


**Figure 10.** Patch clamp current traces (+100 mV) for (a) **8** and (b) **9** ( $0.5 \mu\text{M}$ ) in the planar lipid bilayer in a symmetrical  $\text{NH}_4\text{Cl}$  solution ( $1.0 \text{ M}$ ). Reproduced from ref 49. Copyright 2014 American Chemical Society.

unimolecular tubular conformation for both of them in the bilayer. Because of the squeezing of the surrounding lipid molecules, the peptide chains aggregated to the two sides of the backbones to produce a small pore. Although the exact size of the pore is unclear, it should be smaller than the cavity of the helical backbones (ca.  $1.0 \text{ nm}$  in diameter) because a high  $\text{NH}_4^+$  over  $\text{K}^+$  selectivity was observed, which can be realized only by small pores. Furthermore, more rigid macrocycle-based transporters of larger size were still able to exhibit a good selectivity for  $\text{NH}_4^+$  over  $\text{K}^+$ .<sup>50</sup>

## 7. CONCLUDING REMARKS

Unimolecular channels are complementary to self-assembled multicomponent channels for transmembrane transport of different ions and neutral species. Our results discussed in this Account have shown that highly efficient unimolecular channels can be readily constructed by modifying a rigid backbone with rationally designed side chains. The key is to construct a tubular structure that can span the lipid bilayer. This general strategy can achieve a good balance in generating a long tubular molecular conformation and endowing the channel with the requisite capacity to insert into the bilayer.

Currently we have demonstrated that both porous pillar[ $n$ ]-arenes and hydrogen-bonded aromatic hydrazide helices can serve as rigid frameworks for the design of such families of unimolecular channels. For the first series, future effort will focus on modification of the side chains to create pH-, redox-, or electrochemically responsive channels. For the second series, the helical framework will be replaced with other helical sequences of tunable cavity size to achieve increased transport efficiency and selectivity. It is also noteworthy that the size of the helical aromatic hydrazide backbones is quite large. The fact that this series of channels can achieve a good selectivity for different alkali cations and  $\text{NH}_4^+$  well illustrates the squeezing effect of the lipid molecules for the flexible chains of the inserted channels, which allows the formation of small but tunable pores from large rigid frameworks. With this effect in view, many large, rigid cyclophanes may also be utilized for the design of new channels.

## AUTHOR INFORMATION

### Corresponding Author

\*Phone: (86)-021-65105744. Fax: (86)-021-65105744. E-mail: houjl@fudan.edu.cn.

### Notes

The authors declare no competing financial interest.

## Biographies

**Wen Si** received her B.S. from China Southwest University and her Ph.D. from Fudan University with Professor Jun-Li Hou. Since September 2014, she has been a research associate in the same group and supports the studies on artificial channels.

**Pengyang Xin** obtained his M.S. from Henan Normal University in 2012 and is currently a Ph.D. candidate at the Department of Chemistry of Fudan University, supervised by Professors Jun-Li Hou and Zhan-Ting Li.

**Zhan-Ting Li** received his B.S. from Zhengzhou University and his Ph.D. from Shanghai Institute of Organic Chemistry (SIOC), Chinese Academy of Sciences, with Qing-Yun Chen. He did postdoctoral research with Jan Becher at the University of South Denmark and Steven C. Zimmerman at the University of Illinois at Urbana-Champaign. From 2003 to 2010 he was a professor at SIOC. Currently he is a professor at the Department of Chemistry of Fudan University. His research interests include biomimetic structures and transporters and conjugated and porous supramolecular structures.

**Jun-Li Hou** obtained his B.S. from Hubei University and his Ph.D. from Shanghai Institute of Organic Chemistry (SIOC), Chinese Academy of Sciences, with Professor Zhan-Ting Li. After two years of postdoctoral research at The Scripps Research Institute with Professor Julius Rebek, he joined the Department of Chemistry of Fudan University in 2008, where he currently is a full professor of organic chemistry. His research focuses on the construction of functional supramolecular systems, particularly transmembrane channels and biosensors.

## ACKNOWLEDGMENTS

This research was supported by the National Natural Science Foundation of China (21422202), MOST (2013CB834501), the Ministry of Education of China (IRT1117), STCSM (13NM1400200), and the Open Project of the State Key Laboratory of Supramolecular Structures and Materials (sklssm201508). We express our sincere gratitude to the members and collaborators of our laboratories whose contributions are reflected in the cited references.

## REFERENCES

- (1) Hille, B. *Ionic Channels of Excitable Membranes*, 3rd ed.; Sinauer Associates: Sunderland, MA, 2001; pp 1–2.
- (2) Tabushi, I.; Kuroda, Y.; Yokota, K. A,B,D,F-tetrasubstituted  $\beta$ -cyclodextrin as artificial channel compound. *Tetrahedron Lett.* **1982**, *23*, 4601–4604.
- (3) Matile, S.; Fyles, T. Transport across membranes. *Acc. Chem. Res.* **2013**, *46*, 2741–2742.
- (4) Matile, S.; Sakai, N.; Hennig, A. Transport Experiments in Membranes. In *Supramolecular Chemistry: From Molecules to Nanomaterials*; Gale, P. A., Steed, J. W., Eds.; Wiley: Chichester, U.K., 2012; Vol. 2, pp 473–500.
- (5) Chui, J. K. W.; Fyles, T. M. Ionic conductance of synthetic channels: analysis, lessons, and recommendations. *Chem. Soc. Rev.* **2012**, *41*, 148–175.
- (6) Gokel, G. W.; Murillo, O. Synthetic organic chemical models for transmembrane channels. *Acc. Chem. Res.* **1996**, *29*, 425–432.
- (7) Montenegro, J.; Ghadiri, M. R.; Granja, J. R. Ion channel models based on self-assembling cyclic peptide nanotubes. *Acc. Chem. Res.* **2013**, *46*, 2955–2965.
- (8) Zhao, Y.; Cho, H.; Widanapathirana, L.; Zhang, S. Conformationally controlled oligocholate membrane transporters: learning through water play. *Acc. Chem. Res.* **2013**, *46*, 2763–2772.

- (9) Kaucher, M. S.; Harrell, W. A.; Davis, J. T. A unimolecular G-quadruplex that functions as a synthetic transmembrane Na<sup>+</sup> transporter. *J. Am. Chem. Soc.* **2006**, *128*, 38–39.
- (10) Li, X.; Wu, Y.-D.; Yang, D.  $\alpha$ -Aminoxy acids: new possibilities from foldamers to anion receptors and channels. *Acc. Chem. Res.* **2008**, *41*, 1428–1438.
- (11) Webb, S. J. Supramolecular approaches to combining membrane transport with adhesion. *Acc. Chem. Res.* **2013**, *46*, 2878–2887.
- (12) Fyles, T. M. How do amphiphiles form ion-conducting channels in membranes? Lessons from linear oligoesters. *Acc. Chem. Res.* **2013**, *46*, 2847–2855.
- (13) Urry, D. W.; Goodall, M. C.; Glickson, J. D.; Mayers, D. F. The gramicidin A transmembrane channel: characteristics of head-to-head dimerized  $\pi_{(L,D)}$  helices. *Proc. Natl. Acad. Sci. U.S.A.* **1971**, *68*, 1907–1911.
- (14) Stankovic, C. J.; Heinemann, S. H.; Delfino, J. M.; Sigworth, F. J.; Schreiber, S. L. Transmembrane channels based on tartaric acid–gramicidin A hybrids. *Science* **1989**, *244*, 813–817.
- (15) Schrey, A.; Vescovi, A.; Knoll, A.; Rickert, C.; Koert, U. Synthesis and functional studies of a membrane-bound THF-gramicidin cation channel. *Angew. Chem., Int. Ed.* **2000**, *39*, 900–902.
- (16) Matsubara, A.; Asami, K.; Akagi, A.; Nishino, N. Ion-channels of cyclic template-assembled alamethicins that emulate the pore structure predicted by the barrel-stave model. *Chem. Commun.* **1996**, 2069–2070.
- (17) Woolley, G. A. Channel-forming activity of alamethicin: effects of covalent tethering. *Chem. Biodiversity* **2007**, *4*, 1323–1337.
- (18) Gokel, G. W.; Negin, S. Synthetic ion channels: from pores to biological applications. *Acc. Chem. Res.* **2013**, *46*, 2824–2833.
- (19) Roks, M. F. M.; Nolte, R. J. M. Biomimetic macromolecular chemistry: design and synthesis of an artificial ion channel based on a polymer containing cofacially stacked crown ether rings. Incorporation in dihexadecyl phosphate vesicles and study of cobalt ion transport. *Macromolecules* **1992**, *25*, 5398–5407.
- (20) Voyer, N.; Rohitaille, M. A novel functional artificial ion channel. *J. Am. Chem. Soc.* **1995**, *117*, 6599–6600.
- (21) Winum, J.-Y.; Matile, S. Rigid push–pull oligo(*p*-phenylene) rods: depolarization of bilayer membranes with negative membrane potential. *J. Am. Chem. Soc.* **1999**, *121*, 7961–7962.
- (22) Jullien, L.; Lehn, J.-M. The “chundle” approach to molecular channels synthesis of a macrocycle-based molecular bundle. *Tetrahedron Lett.* **1988**, *29*, 3803–3806.
- (23) Fyles, T. M. Synthetic ion channels in bilayer membranes. *Chem. Soc. Rev.* **2007**, *36*, 335–347.
- (24) Pregel, M. J.; Jullien, L.; Canceill, J.; Lacombe, L.; Lehn, J.-M. Channel-type molecular structures. Part 4. Transmembrane transport of alkali-metal ions by “bouquet” molecules. *J. Chem. Soc., Perkin Trans. 2* **1995**, 417–426.
- (25) Mendoza, J.; Cuevas, F.; Prados, P.; Meadows, E. S.; Gokel, G. W. A synthetic cation-transporting calix[4]arene derivative active in phospholipid bilayers. *Angew. Chem., Int. Ed.* **1998**, *37*, 1534–1537.
- (26) Maulucci, N.; De Riccardis, F.; Botta, C. B.; Casapullo, A.; Cressina, E.; Fregonese, M.; Tecilla, P.; Izzo, I. Calix[4]arene–cholic acid conjugates: a new class of efficient synthetic ionophores. *Chem. Commun.* **2005**, 1354–1356.
- (27) Jeon, Y. J.; Kim, H.; Jon, S.; Selvapalam, N.; Oh, D. H.; Seo, I.; Park, C.-S.; Koh, D.-S.; Kim, K. Artificial ion channel formed by cucurbit[*n*]uril derivatives with a carbonyl group fringed portal reminiscent of the selectivity filter of K<sup>+</sup> channels. *J. Am. Chem. Soc.* **2004**, *126*, 15944–15945.
- (28) Tanaka, Y.; Kobuke, Y.; Sokabe, M. A non-peptide ion channel with K<sup>+</sup> selectivity. *Angew. Chem., Int. Ed. Engl.* **1995**, *34*, 693–694.
- (29) Gokel, G. W.; Mukhopadhyay, A. Synthetic models of cation-conducting channels. *Chem. Soc. Rev.* **2001**, *30*, 274–286.
- (30) Matile, S.; Jentzsch, A. V.; Montenegro, J.; Fin, A. Recent synthetic transport systems. *Chem. Soc. Rev.* **2011**, *40*, 2453–2474.
- (31) Organo, V. G.; Leontiev, A. V.; Sgarlata, V.; Dias, H. V. R.; Rudkevich, D. M. Supramolecular features of calixarene-based synthetic nanotubes. *Angew. Chem., Int. Ed.* **2005**, *44*, 3043–3047.
- (32) Ogoshi, T.; Kanai, S.; Fujinami, S.; Yamagishi, T. A.; Nakamoto, Y. Para-bridged symmetrical pillar[5]arenes: their Lewis acid catalyzed synthesis and host–guest property. *J. Am. Chem. Soc.* **2008**, *130*, 5022–5023.
- (33) Han, C.; Ma, F.; Zhang, Z.; Xia, B.; Yu, Y.; Huang, F. DIBpillar[*n*]arenes (*n* = 5, 6): syntheses, X-ray crystal structures, and complexation with *n*-octyltriethyl ammonium hexafluorophosphate. *Org. Lett.* **2010**, *12*, 4360–4363.
- (34) Xue, M.; Yang, Y.; Chi, X.; Zhang, Z.; Huang, F. Pillararenes, a new class of macrocycles for supramolecular chemistry. *Acc. Chem. Res.* **2012**, *45*, 1294–1308.
- (35) Hu, X.-B.; Chen, Z.; Chen, L.; Zhang, L.; Hou, J.-L.; Li, Z.-T. Pillar[*n*]arenes (*n* = 8–10) with two cavities: synthesis, structures and complexing properties. *Chem. Commun.* **2012**, *48*, 10999–11001.
- (36) Si, W.; Hu, X.-B.; Liu, X.-H.; Fan, R.; Chen, Z.; Weng, L.; Hou, J.-L. Self-assembly and proton conductance of organic nanotubes from pillar[5]arenes. *Tetrahedron Lett.* **2011**, *52*, 2484–2487.
- (37) Nagle, J. F.; Tristram-Nagle, S. Hydrogen bonded chain mechanisms for proton conduction and proton pumping. *J. Membr. Biol.* **1983**, *74*, 1–14.
- (38) Si, W.; Chen, L.; Hu, X.-B.; Tang, G.; Chen, Z.; Hou, J.-L.; Li, Z.-T. Selective artificial transmembrane channels for protons by formation of water wires. *Angew. Chem., Int. Ed.* **2011**, *50*, 12564.
- (39) Agmon, N. The Grothhuss mechanism. *Chem. Phys. Lett.* **1995**, *244*, 456–462.
- (40) Weiss, L. A.; Sakai, N.; Ghebremariam, B.; Ni, C.; Matile, S. Rigid rod-shaped polyols: functional nonpeptide models for transmembrane proton channels. *J. Am. Chem. Soc.* **1997**, *119*, 12142–12149.
- (41) Schnell, J. R.; Chou, J. J. Structure and mechanism of the M2 proton channel of influenza A virus. *Nature* **2008**, *451*, 591–595.
- (42) Hu, X.-B.; Chen, Z.; Tang, G.; Hou, J.-L.; Li, Z.-T. Single-molecular artificial transmembrane water channels. *J. Am. Chem. Soc.* **2012**, *134*, 8384–8387.
- (43) Burykin, A.; Warshel, A. What really prevents proton transport through aquaporin? Charge self-energy versus proton wire proposals. *Biophys. J.* **2003**, *85*, 3696–3706.
- (44) Barboiu, M.; Gilles, A. From natural to bioassisted and biomimetic artificial water channel systems. *Acc. Chem. Res.* **2013**, *46*, 2814–2823.
- (45) Chen, L.; Si, W.; Zhang, L.; Tang, G.; Li, Z.-T.; Hou, J.-L. Chiral selective transmembrane transport of amino acids through artificial channels. *J. Am. Chem. Soc.* **2013**, *135*, 2152–2155.
- (46) Si, W.; Li, Z.-T.; Hou, J.-L. Voltage-driven reversible insertion into and leaving from a lipid bilayer: tuning transmembrane transport of artificial channels. *Angew. Chem., Int. Ed.* **2014**, *53*, 4578–4581.
- (47) Lai, H. C.; Jan, L. Y. The distribution and targeting of neuronal voltage-gated ion channels. *Nat. Rev. Neurosci.* **2006**, *7*, 548–562.
- (48) Hou, J.-L.; Shao, X.-B.; Chen, G.-J.; Zhou, Y.-X.; Jiang, X.-K.; Li, Z.-T. Hydrogen bonded oligohydrazide foldamers and their recognition for saccharides. *J. Am. Chem. Soc.* **2004**, *126*, 12386–12394.
- (49) Xin, P.; Zhu, P.; Su, P.; Hou, J.-L.; Li, Z.-T. Hydrogen-bonded helical hydrazide oligomers and polymer that mimic the ion transport of gramicidin A. *J. Am. Chem. Soc.* **2014**, *136*, 13078–13081.
- (50) Xin, P.; Zhang, L.; Su, P.; Hou, J.-L.; Li, Z.-T. Hydrazide macrocycles as effective transmembrane channels for ammonium. *Chem. Commun.* **2015**, *51*, 4819–4822.